

NASA Contractor Report 3313

On One-Dimensional Stretching Functions for Finite- Difference Calculations

Marcel Vinokur
University of Santa Clara
Santa Clara, California

Prepared for
Ames Research Center
under Grant NSG-2086

NASA

National Aeronautics
and Space Administration

**Scientific and Technical
Information Branch**

1980

INDEX

<i>List of Figures</i>	i
<i>Abstract</i>	ii
I. INTRODUCTION	1
II. TRUNCATION ERROR ANALYSIS FOR ONE-DIMENSIONAL STRETCHING FUNCTIONS	4
III. A GENERAL TWO-SIDED STRETCHING FUNCTION	9
IV. A GENERAL INTERIOR STRETCHING FUNCTION	18
V. CONCLUDING REMARKS	22
VI. REFERENCES	27
APPENDIX A: EVALUATION OF ANTI-SYMMETRIC TWO-SIDED STRETCHING FUNCTIONS	28
APPENDIX B: INVERSION OF $y = \sinh x/x$	34
APPENDIX C: INVERSION OF $y = \sin x/x$	38
APPENDIX D: SOLUTION CHARACTERISTICS OF THE TWO-SIDED STRETCHING FUNCTION DERIVED FROM $w = \tanh z$	40
APPENDIX E: EVALUATION OF ANTI-SYMMETRIC INTERIOR STRETCHING FUNCTIONS	48

List of Figures

Figure 1.	Two-Sided Stretching Function for $S_0 = 100$ and Different Values of S_1	26
Figure D.1.	Solution Characteristics of Two-Sided Stretching Functions Derived from $w = \tanh z$	46
Figure D.2.	Locus of Solution in z-Plane	47

ABSTRACT

The class of one-dimensional stretching functions used in finite-difference calculations is studied. For solutions containing a highly localized region of rapid variation, simple criteria for a stretching function are derived using a truncation error analysis. These criteria are used to investigate two types of stretching functions. One is an interior stretching function, for which the location and slope of an interior clustering region are specified. The simplest such function satisfying the criteria is found to be one based on the inverse hyperbolic sine. It was first employed by Thomas et al. The other type of function is a two-sided stretching function, for which the arbitrary slopes at the two ends of the one-dimensional interval are specified. The simplest such general function is found to be one based on the inverse tangent. The special case where the slopes were both equal and greater than one was first employed by Roberts. The general two-sided function has many applications in the construction of finite-difference grids. An example of such an application is found in one of the references.

I. INTRODUCTION

Finite-difference calculations of fluid flow problems are best carried out using an equispaced grid in a rectangular (or cubic) computational domain, with the flow variables and components of the position vector as dependent variables, and boundary conditions applied at the edges (or faces) of the domain. In order to minimize the number of grid points required for a given accuracy, one seeks boundary-fitted coordinate transformations that cluster points in regions where the dependent variables undergo rapid variation. These regions may be due to body geometry (very large curvatures or corners), compressibility (entropy layers, shock waves and contact discontinuities), and viscosity (boundary layers and shear layers). A complex flow may thus contain a variety of such regions of various length scales, and often of unknown location. An ideal grid would adjust with each time or iteration step to maintain optimum clustering. Such adaptive grid methods, which involve the solution of auxiliary equations, have been developed for one-dimensional problems (refs. 1-3). Their extension to complex multi-dimensional flows is a difficult problem, particularly when the regions requiring clustering do not have simple topological properties required by a finite-difference grid.

There are many practical problems in which the locations and length scales of regions of rapid variation can be estimated a priori (e.g., known geometry, attached boundary layers, simple shock wave configurations). In these cases the clustering can be incorporated in automatic grid generators which solve an elliptic boundary-value problem (refs. 4-6). The distribution of grid points on the boundaries is then normally prescribed algebraically, using one-dimensional stretching functions. (Here, stretching function refers to any transformation involving stretching or clustering). It is also possible to employ stretching functions to obtain a clustered grid from an unclustered grid by applying clustering to one coordinate family only. For some simple geometries, one can construct entire clustered grids purely algebraically, using only one-dimensional stretching functions.

The simplest class of one-dimensional stretching functions is that involving two parameters. In interior stretching functions, the parameters are the location and slope of a single clustering region. In two-sided stretching functions, the slopes at the two ends of the one-dimensional interval are specified. The anti-symmetric two-sided stretching function (with the same slope at each end) is of special interest, since the portion from the midpoint to either end defines a one-sided stretching function (with zero curvature at the other end). A one-sided stretching function can also be obtained as a special case of the interior stretching function, by locating the clustering region at one end. Since the clustered end has zero curvature in this case, these two one-sided stretching functions are of a different nature.

An interior stretching function based on the inverse hyperbolic sine was employed by Thomas, Vinokur, Bastianon, and Conti (ref. 7) in a numerical solution of inviscid supersonic flow over a blunt delta wing with elliptical cross section. The function was used to cluster points on the body at the vertices of very eccentric ellipses. The one-sided version clustered points in the flow near the body surface to resolve the entropy layer due to the bow shock. No derivation of the stretching function was given, and the clustering parameter appearing in it was not related to the length scales of regions of rapid variation in physical space.

An anti-symmetric two-sided stretching function of a logarithmic type was employed by Roberts (ref. 8) to study boundary layer flows. The heuristic derivation of the function avoided consideration of the truncation errors associated with finite-difference approximations. While this function has been used successfully in many flow calculations, there is a need for a general two-sided function which allows arbitrary stretching or clustering to be specified independently at each end. An application would be problems in which the appropriate length scales requiring clustering are significantly different at the two ends. Another application is the distribution of grid points on a curve which is

defined piecewise, where continuity of grid spacing is desired at the ends of the piecewise segments. A third application is the use of such a function as a blending or interpolating function to construct two and three-dimensional grids using one-dimensional stretching functions and shearing transformation. The construction of a single, well-ordered grid for wing body flows by Vinokur (ref. 9) is an example of these applications.

The present work has two objectives. One is to obtain simple, rational criteria for one-dimensional stretching functions, by considering the truncation errors inherent in finite-difference approximations. The functions introduced by Thomas et al and Roberts will be found to be the simplest ones satisfying these criteria. The other objective is to derive a simple form of the general two-sided stretching function.

II. TRUNCATION ERROR ANALYSIS FOR ONE-DIMENSIONAL STRETCHING FUNCTIONS

An exact analysis of the truncation error inherent in a finite-difference calculation would require knowledge of the equation being solved and the finite difference approximation that is used. Here we are concerned with the special situation where the solution contains a highly localized region of rapid variation with respect to some coordinate, and we seek approximate criteria for a stretching function that will be independent of the equation or difference algorithm. The quantities that are approximated are in general non-linear functions of the unknowns and their spatial derivatives. The error analysis will be performed in terms of the fractional truncation errors for the spatial derivatives.

Let $\vec{r}(\bar{t})$ be the equation describing a $\bar{\xi}$ -coordinate curve, where \bar{t} is any parameter that varies smoothly with arc length. If A and B denote the ends of the curve, we introduce the normalized variables

$$t = (\bar{t} - \bar{t}_A) / (\bar{t}_B - \bar{t}_A) \quad (1a)$$

$$\text{and } \xi = (\bar{\xi} - \bar{\xi}_A) / (\bar{\xi}_B - \bar{\xi}_A), \quad (1b)$$

ranging from 0 to 1. For simplicity, all partial derivatives with respect to ξ or t will be written as total derivatives. Let $\phi(t)$ be any function of the unknowns. Outside of the region where $d\phi/dt = 0$, we can define a natural length scale of the variation of ϕ with respect to t as

$$L_{\phi t} = \left| \frac{d\phi}{dt} / \frac{d^2\phi}{dt^2} \right|. \quad (2)$$

Since the components of \vec{r} also enter as dependent variables in the calculation of metrics and Jacobians, we similarly define the natural length scale of the variation of \vec{r} with respect to t as

$$L_{rt} = \left| \frac{d\vec{r}}{dt} / \left| \frac{d^2\vec{r}}{dt^2} \right| \right|. \quad (3)$$

Note that if t is proportional to arc length, then L_{rt} is precisely the radius of curvature, normalized by the length of the curve.

Assume first that t is used as the normalized computational variable (i.e. $\xi = t$), with Δt as the uniform grid spacing. Let $\delta\phi/\delta t$ denote the finite difference approximation to $d\phi/dt$. Using equation (2), one can write any first order accurate approximation as

$$\frac{\delta\phi}{\delta t} = \frac{d\phi}{dt} [1 + O(L_{\phi t}^{-1} \Delta t)]. \quad (4)$$

Similarly, the approximation to $d\vec{r}/dt$ can be written as

$$\frac{\delta\vec{r}}{\delta t} = \frac{d\vec{r}}{dt} [1 + O(L_{rt}^{-1} \Delta t)]. \quad (5)$$

If $L_{\phi t}^{-1}$ or L_{rt}^{-1} became very large in some localized region, then a prohibitively small Δt would be required to obtain a desired fractional truncation error. Outside of the localized region, the excessive number of grid points would be wasted. The obvious remedy is to seek a new computational variable ξ for which $L_{\phi\xi}^{-1}$ and $L_{r\xi}^{-1}$ remain of $O(1)$, even though $L_{\phi t}^{-1}$ or L_{rt}^{-1} could be locally very large.

With the aid of the identities

$$\frac{d\phi}{d\xi} = \frac{d\phi}{dt} \frac{dt}{d\xi} \quad (6)$$

and

$$\frac{d^2\phi}{d\xi^2} = \frac{d^2\phi}{dt^2} \left(\frac{dt}{d\xi}\right)^2 + \frac{d\phi}{dt} \frac{d^2t}{d\xi^2}, \quad (7)$$

and definition (2), one can easily show that

$$L_{\phi\xi}^{-1} \leq L_{\phi t}^{-1} \frac{dt}{d\xi} + L_{t\xi}^{-1}. \quad (8)$$

Similarly, using definition (3), one obtains the inequality

$$L^{-1}_{r\xi} \leq L^{-1}_{rt} \frac{dt}{d\xi} + L^{-1}_{t\xi}. \quad (9)$$

One criterion for the stretching function $\xi(t)$ is therefore

$$L^{-1}_{t\xi} = O(1), \quad (10)$$

In addition, we require that

$$L^{-1}_{\phi t} \frac{dt}{d\xi} = O(1), \quad (11)$$

and

$$L^{-1}_{rt} \frac{dt}{d\xi} = O(1). \quad (12)$$

Consider the case where $L^{-1}_{\phi t}$ is very large in some localized region. It follows from equation (11) that

$$\frac{dt}{d\xi} = O(L_{\phi t}) \quad (13)$$

in that region. Since $L^{-1}_{\phi t}$ remains large over an interval whose thickness is of $O(L_{\phi t})$, we require that $dt/d\xi$ remains small over that interval. Furthermore, since $L^{-1}_{\phi t} = O(1)$ outside of the localized region, it follows from equation (11) that $dt/d\xi = O(1)$, i.e. that $dt/d\xi$ does not become large anywhere. But these two additional requirements are satisfied if condition (10) is valid. Noting that

$$\frac{d}{dt} \left(\frac{dt}{d\xi} \right) = \frac{d^2 t}{d\xi^2} / \left(\frac{dt}{d\xi} \right), \quad (14)$$

it follows upon integration over a finite interval Δt that

$$\left| \Delta \left(\frac{dt}{d\xi} \right) \right| \leq (L^{-1}_{t\xi})_{\max} \Delta t. \quad (15)$$

Applying equation (15) to the localized region, for which $\Delta t = O(L_{\phi t})$, we find, using equation (10), that

$$\left| \Delta \left(\frac{dt}{d\xi} \right) \right| = O(L_{\phi t}). \quad (16)$$

Thus equation (13) is satisfied over the entire localized region. Letting $\Delta t = 1$ in equation (15), we see that $dt/d\xi = O(1)$ is satisfied over the complete range of t . In the event that L_{rt}^{-1} is larger than $L_{\phi t}^{-1}$ in the localized region, then condition (13) is replaced by

$$\frac{dt}{d\xi} = O(L_{rt}). \quad (17)$$

The above analysis is easily extended to higher order finite-difference approximations, as well as the treatment of higher derivatives. In order to consider fractional truncation errors due to a second-order accurate approximation to $d\phi/dt$ (and also for regions where $d^2\phi/dt^2 = 0$), it is appropriate to define a different length scale of the variation of ϕ with respect to t as

$$\bar{L}_{\phi t} = \left| \frac{d\phi}{dt} / \frac{d^3\phi}{dt^3} \right|^{1/2}. \quad (18)$$

We now require that $\bar{L}_{\phi\xi}^{-1}$ remains of $O(1)$, even though $\bar{L}_{\phi t}^{-1}$ could be locally very large. Using the identity

$$\frac{d^3\phi}{d\xi^3} = \frac{d^3\phi}{dt^3} \left(\frac{dt}{d\xi} \right)^3 + 3 \frac{d^2\phi}{dt^2} \frac{dt}{d\xi} \frac{d^2t}{d\xi^2} + \frac{d\phi}{dt} \frac{d^3t}{d\xi^3}, \quad (19)$$

we obtain the inequality

$$\bar{L}_{\phi\xi}^{-2} \leq (\bar{L}_{\phi t}^{-1} \frac{dt}{d\xi})^2 + 3 L_{\phi t}^{-1} \frac{dt}{d\xi} L_{t\xi}^{-1} + \bar{L}_{t\xi}^{-2}. \quad (20)$$

In addition to satisfying equation (10), the stretching function $\xi(t)$ must satisfy

$$\bar{L}_{t\xi}^{-1} = O(1). \quad (21)$$

Also, if $\bar{L}_{\phi t}^{-1}$ is larger than $L_{\phi t}^{-1}$ in the localized region, condition (13) must be replaced by

$$\frac{dt}{d\xi} = 0 \left(\bar{L}_{\phi t} \right). \quad (22)$$

A first order finite difference approximation to $d^2\phi/dt^2$ requires the introduction of the length scale

$$\tilde{L}_{\phi t} = \left| \frac{d^2\phi/dt^2}{d^3\phi/dt^3} \right|. \quad (23)$$

Combining equations (2), (18), and (23), we see that

$$\tilde{L}_{\phi \xi}^{-1} = \bar{L}_{\phi \xi}^{-2} / L_{\phi \xi}^{-1}. \quad (24)$$

Thus conditions (10), (21), and (13) or (22) are sufficient to guarantee that $\tilde{L}_{\phi \xi}^{-1}$ remains of $O(1)$. The length scale $\tilde{L}_{\phi t}$ is also the appropriate one to use at a point where $d\phi/dt = 0$. At such a point, using equations (7) and (19), we obtain the relation

$$\tilde{L}_{\phi \xi}^{-1} \leq \tilde{L}_{\phi t}^{-1} \frac{dt}{d\xi} + 3 L_{t \xi}^{-1}. \quad (25)$$

The criteria for $\xi(t)$ is again equation (10), with equation (13) replaced by

$$\frac{dt}{d\xi} = 0 \left(\tilde{L}_{\phi t} \right) \quad (26)$$

if the localized region of rapid variation occurs around the point $d\phi/dt = 0$. Conditions (22) and (26) are to be replaced by analogous ones containing \bar{L}_{rt} and \tilde{L}_{rt} , if these are the more significant length scales.

In summary, one first defines length scales appropriate to the difference approximation and the location of the region of rapid variation. The criteria for the stretching function $\xi(t)$ can be stated as:

1. All the inverse length scales of the variation of t with respect to ξ must be at most of order one throughout the range of t .
2. The slope $dt/d\xi$ must be of the order of the minimum length scale of the variation of ϕ or \vec{r} with respect to t in the localized region of rapid variation.

These criteria will insure that most of the grid points will be concentrated in the localized region of rapid variation, with a sufficient number of points left in the remainder of the domain. The criteria will be used to investigate the two-parameter stretching functions of the next two sections.

III. A GENERAL TWO-SIDED STRETCHING FUNCTION

In this section we derive a general two-sided stretching function $\xi(t; s_0, s_1)$, where ξ and t are normalized variables defined by equation (1), and the parameters s_0 and s_1 are dimensionless slopes defined as

$$s_0 = \frac{d\xi}{dt} (0) \quad (27a)$$

and

$$s_1 = \frac{d\xi}{dt} (1). \quad (27b)$$

In order to be useful for constructing finite-difference grids, the function must be monotonic, and satisfy conditions (10) and (21) even if s_0 or s_1 becomes very large. For a general range of applications, it would be desirable for the function to be simple, invertible, and to vary continuously over the complete ranges of s_0 and s_1 .

An attractive candidate for such a stretching function is a scaled portion of a single, universal function $w(z)$. For a given s_0 and s_1 , the stretching function will be obtained by properly scaling the portion of the universal function from corresponding points z_0 and z_1 . An additional requirement is that the unnormalized function $\bar{\xi}(\bar{t})$ be independent of the designation

of a particular end as A or B. One can easily show that this restricts the universal function to be odd, i.e.

$$w(-z) = -w(z).$$

The simplest odd, monotonic, invertible functions are $\sinh z$ and $\tanh z$. Their hyperbolic relatives are produced by letting z be complex. The inverse functions are formed by associating z with either t or ξ . One can determine whether either universal function is suitable as a basis for a stretching function by applying conditions (10) and (21) for very large s_0 or s_1 . Actually, the most extreme test occurs for the simpler anti-symmetric cases $s_0 = s_1$, which corresponded to $z_0 = -z_1$, with z being either real or pure imaginary.

An evaluation of the anti-symmetric two-sided stretching functions obtained from $\sinh z$ and $\tanh z$ is carried out for the case $s_0 = s_1 > 1$ in Appendix A. Only $\tanh z$ produces a stretching function satisfying conditions (10) and (21), with the inverse length scales being logarithmically of $O(1)$. The stretching function $\xi(t)$ is a scaled portion of the inverse hyperbolic tangent. Expressing the hyperbolic tangent as a logarithm, we obtain exactly the function derived by Roberts (ref. 8). It turns out that $L_{t\xi}^{-1}$ is a piecewise linear function of t , a property that was used by Roberts to define his function. This suggests a related stretching function, for which $L_{t\xi}^{-1}$ is a piecewise linear function of ξ . The corresponding universal function is the error function $\operatorname{erf} z$. The associated stretching function is also analyzed in Appendix A, and found to satisfy conditions (10) and (21). However, it is not invertible, and has larger maximum inverse length scales than the former stretching function.

On the basis of the above considerations, the universal function $w = \tanh z$ will be used to obtain a stretching function for arbitrary s_0 and s_1 . Introducing the ranges

$$\Delta z = z_1 - z_0 \tag{28}$$

and

$$\Delta w = \tan z_1 - \tan z_0, \quad (29)$$

we can define the normalized variables

$$\xi = (z - z_0)/\Delta z \quad (30)$$

and

$$t = (\tan z - \tan z_0)/\Delta w. \quad (31)$$

The slope of the stretching function is then given by

$$\frac{d\xi}{dt} = \frac{\Delta w}{\Delta z} \cos^2 z. \quad (32)$$

Using the trigonometric identity

$$\tan z_1 - \tan z_0 = \frac{\sin(z_1 - z_0)}{\cos z_1 \cos z_0}, \quad (33)$$

we find for the parameters s_0 and s_1 the relations

$$s_0 = \frac{\sin \Delta z \cos z_0}{\Delta z \cos z_1} \quad (34)$$

and

$$s_1 = \frac{\sin \Delta z \cos z_1}{\Delta z \cos z_0}. \quad (35)$$

This suggests introducing the new parameters

$$B = \sqrt{s_0 s_1} \quad (36)$$

and

$$A = \sqrt{s_0/s_1}. \quad (37)$$

The parameters A and B can then be expressed in terms of z_0 and z_1 as

$$B = \frac{\sin \Delta z}{\Delta z} \quad (38)$$

and

$$A = \frac{\cos z_0}{\cos z_1} \quad (39)$$

Using the cosine sum identity, we can also write equation (39) as

$$A = \cos \Delta z + \tan z_1 \sin \Delta z \quad (40a)$$

and

$$1/A = \cos \Delta z - \tan z_0 \sin \Delta z. \quad (40b)$$

For a given value of B, Δz is obtained by solving equation (38). Equation (40) can then be solved to obtain z_0 and Δw for a given value of A. The stretching function obtained from equations (30) and (31) can then be written as

$$t = \frac{\tan(\xi \Delta z + z_0) - \tan z_0}{\Delta w} \quad (41)$$

While equation (41) is a formal expression for the general stretching function, it cannot be used for calculations in its present form. Depending on the value of B, Δz and Δw are either real or pure imaginary. For certain ranges of A and B, z_0 can become complex. Using the tangent sum identity and equation (39), we can eliminate z_0 from equation (41) and obtain instead

$$t = \frac{\tan \xi \Delta z}{A \sin \Delta z + (1 - A \cos \Delta z) \tan \xi \Delta z} \quad (42)$$

This can be further simplified by noting that $A = 1$ corresponds to the anti-symmetric solution which was analyzed in Appendix A. Let us denote this solution as $u(\xi)$. Setting $A = 1$ in equation (42), and using the tangent sum identity, we obtain

$$u = 1/2 + \frac{\tan [\Delta z (\xi - 1/2)]}{2 \tan (\Delta z/2)} \quad (43)$$

In terms of u , equation (42) then takes the simple form

$$t = \frac{u}{A + (1 - A)u}, \quad (44)$$

which can be readily inverted as

$$u = \frac{t}{(1/A) + (1 - 1/A)t}. \quad (45)$$

Note that both $u(t)$ and its inverse can be obtained as scaled portions of a rectangular hyperbola. For each function, the slopes at the two ends are A and $1/A$, respectively. Finally, we observe that for calculational purposes, equations (44) and (45) are well behaved in the neighborhood of $A = 1$.

We thus have the remarkable result that one essentially needs to know only the anti-symmetric stretching function for the geometric mean of the slopes S_0 and S_1 . The square root of the ratio of those slopes determines an additional simple transformation which produces the desired stretching function. Since both equations (43) and (44) are invertible, the resultant stretching function is also invertible. The key trigonometric property making this result possible is that the tangent of a sum is a rational function of the individual tangents. By contrast, the sine of a sum involves the individual sines and cosines, and is not expressible as a rational function of sines alone. An analysis of a stretching function based on $w = \sin z$ has been carried out, but is not presented here. The parameters corresponding to B and A turn out to be the arithmetic mean and difference of the two slopes. A separation into two functions corresponding to equations (43) and (44) is not possible, and one must use the direct form corresponding to equations (41) and (42). For $B > 1$, the inversion involves the solution of a quadratic equation, and the sign of A must be tested in order to choose the appropriate root. It is indeed serendipity that the tangent function

dictated by truncation error considerations is also the much simpler one for constructing a general two-sided stretching function.

The calculation of the anti-symmetric function depends on the size of B. If $B > 1$, it follows from equation (38) that z is imaginary and we obtain the results (previously obtained in Appendix A)

$$B = \frac{\sinh \Delta y}{\Delta y} \quad (46)$$

and

$$u = 1/2 + \frac{\tanh [\Delta y (\xi - 1/2)]}{2 \tanh (\Delta y/2)} \quad (47)$$

The inversion of equation (47) yields

$$\xi = 1/2 + \frac{\tanh^{-1} [(2u - 1) \tanh (\Delta y/2)]}{2\Delta y} \quad (48)$$

Note that the hyperbolic tangent and its inverse can be expressed in terms of exponentials and a logarithm, respectively.

For $B < 1$, Δz is real, and the corresponding results are

$$B = \frac{\sin \Delta x}{\Delta x}, \quad (49)$$

$$u = 1/2 + \frac{\tan [\Delta x (\xi - 1/2)]}{2 \tan (\Delta x/2)}, \quad (50)$$

and
$$\xi = 1/2 + \frac{\tan^{-1} [(2u-1) \tan (\Delta x/2)]}{2\Delta x} \quad (51)$$

When B is very near one, both of the above formulations break down, since Δx and Δy approach zero. The appropriate expressions are obtained by expanding equations (49) and (50) in powers of Δx . To first order in $B-1$, one obtains

$$u \approx \xi [1 + 2(B - 1) (\xi - .5)(1 - \xi)] \quad (52)$$

and

$$\xi \approx u [1 - 2(B - 1) (u - .5)(1 - u)]. \quad (53)$$

By scaling half of the above functions, one obtains the one-sided stretching functions with s_0 given at $t = 0$ and zero curvature at $t = 1$.

The results are:

$$\frac{s_0 > 1}{\quad} \quad s_0 = \frac{\sinh 2\Delta y}{2\Delta y}, \quad (54)$$

$$t = 1 + \frac{\tanh [\Delta y(\xi - 1)]}{\tanh \Delta y}, \quad (55)$$

and

$$\xi = 1 + \frac{\tanh^{-1} [(t - 1)\tanh \Delta y]}{\Delta y}. \quad (56)$$

$$\frac{s_0 < 1}{\quad} \quad s_0 = \frac{\sin 2\Delta x}{2\Delta x}, \quad (57)$$

$$t = 1 + \frac{\tan [\Delta x(\xi - 1)]}{\tan \Delta x}, \quad (58)$$

$$\xi = 1 + \frac{\tan^{-1} [(t - 1)\tan \Delta x]}{\Delta x}. \quad (59)$$

$$\frac{s_0 \approx 1}{\quad} \quad t = \xi [1 - .5(s_0 - 1)(1 - \xi)(2 - \xi)] \quad (60)$$

$$\text{and} \quad \xi = t [1 + .5(s_0 - 1)(1 - t)(2 - t)]. \quad (61)$$

The two-sided stretching functions for $B > 1$ and one sided stretching function for $s_0 > 1$ require the inversion of the function

$$y = \sinh x/x. \quad (62)$$

An approximate analytic representation of the inverse function $x = f(y)$, valid over the range of y required by a stretching function, is derived in Appendix B. The results are as follows:

For $y < 2.7829681$

$$x = \sqrt{6y} (1 - .15\bar{y} + .057321429\bar{y}^2 - .024907295\bar{y}^3 + .0077424461\bar{y}^4 - .0010794123\bar{y}^5), \quad (63)$$

where

$$\bar{y} = y - 1. \quad (64)$$

For $y > 2.7829681$

$$x = v + (1 + 1/v) \log(2v) - .02041793 + .24902722w \\ + 1.9496443w^2 - 2.6294547w^3 + 8.56795911w^4, \quad (65)$$

where $v = \log y \quad (66)$

and $w = 1/y - .028527431. \quad (67)$

The maximum magnitude of the fractional error in y as defined by equation (B.2) is .000267732 for $1 < y < 69.64$. The magnitude of the error reaches .00083 at $y = 120.5$. These errors are small enough so that the grids constructed by the resultant stretching functions will exhibit slope discontinuities that are negligible within the accuracy of any practical finite-difference approximation.

The two-sided stretching function for $B < 1$ and one-sided stretching function for $s_0 < 1$ require the inversion of the function

$$y = \sin x/x. \quad (68)$$

An approximate analytic representation of the inverse function is derived in Appendix C. The results are as follows:

For $y < .26938972$ (69)

$$x = \pi [1 - y + y^2 - (1 + \pi^2/6)y^3 + 6.794732y^4 \\ - 13.205501y^5 + 11.726095y^6].$$

For $.26938972 < y < 1$ (70)

$$x = \sqrt{6\bar{y}} (1 + .15\bar{y} + .057321429\bar{y}^2 + .048774238\bar{y}^3 \\ - .053337753\bar{y}^4 + .075845134\bar{y}^5),$$

where (71)

$$\bar{y} = 1 - y.$$

The maximum magnitude of the fractional error in y defined by equation (C.2) is .00019717, which is small enough for numerical applications.

While it is appealing to view the general two-sided stretching function as a distortion of an anti-symmetric stretching function via equations (43) and (44), there are advantages in looking at the more basic forms of the solution given by equations (41) and (42). If efficiency in terms of operations count is important, then the optimum form for the case $B > 1$ is derived from equation (42), as either

$$t = \frac{\tanh \xi \Delta y}{\sinh \Delta y + (1 - A \cosh \Delta y)} \quad (72a)$$

$$\text{or } t = \frac{e^{2\xi \Delta y} - 1}{e^{2\xi \Delta y} (1 - Ae^{-\Delta y}) + Ae^{\Delta y} - 1}. \quad (72b)$$

The most efficient form for the case $B < 1$ is equation (41) with z replaced by x throughout.

It is also instructive to study the general solution (41), and see how it reduces to different real representations for various ranges of A and B . This is carried out in Appendix D. It is easy to demonstrate that for $B < 1$, the solution is a scaled portion of a tangent, while for $B = 1$ it is a scaled portion of a rectangular hyperbola. For $B > 1$ (and the corresponding Δy given by equation (46), the representation depends on the value of A . As shown in Appendix D, if $\exp(-\Delta y) < A < \exp(\Delta y)$, the solution is a scaled portion of a hyperbolic tangent. Outside of that range the corresponding function is the hyperbolic cotangent, while on the boundary it is the exponential function.

When $A = 1$, the stretching function is anti-symmetric, and the solution curve contains an inflection point. As A departs from one, the inflection point moves towards one end, and eventually could disappear. It is shown in Appendix D that an inflection point will be present if $1/\cosh \Delta y < A < \cosh \Delta y$ for $B > 1$, and $\cos \Delta x < A < 1/\cos \Delta x$ for $B < 1$. If $B < 2/\pi$, the solution must always contain an inflection point. Figure D.1 is a log-log plot of the B vs A plane, showing the inflection point regions, as well

as the boundaries for the various real representations of the solution. Another way to study equation (41) is to follow the path of the solution in the complex z -plane. This is also carried out in Appendix D, with the results plotted in Figure D.2. The plot shows clearly the transition from one representation to another as the parameters A and B are varied.

A typical set of curves for the two-sided stretching function $t(\xi)$ is shown in figure 1 for $s_0 = 100$, and for values of s_1 ranging from .1 to 100. The figure shows the smooth transition from solutions containing an inflection point, for large s_1 , to those without an inflection point for small s_1 . Note that the high concentration of points at the two ends for $s_1 = 100$ still leaves a sufficient number of points to resolve the central region.

IV. A GENERAL INTERIOR STRETCHING FUNCTION

In this section we derive a general interior stretching function $\xi(t; s_i, t_i)$, where s_i is the dimensionless slope at the inflection point t_i , i.e.

$$s_i = \frac{d\xi}{dt} (t_i) \quad (73)$$

and
$$\frac{d^2\xi}{dt^2} (t_i) = 0 \quad (0 \leq t_i \leq 1). \quad (74)$$

We limit our consideration to $s_i > 1$, which is the only case of practical interest. We again look for a function which is a scaled portion of an odd universal function $w(z)$. As in Section III, the simple functions $\sinh z$ and $\tanh z$ are considered first, and conditions (10) and (21) are examined for the anti-symmetric case ($t_i = 1/2$) when s_i is very large. The evaluation is carried out in Appendix E, and $\sinh z$ is found to produce an appropriate function with inverse length scales that are logarithmically of $O(1)$. The stretching function $\xi(t)$ is a scaled portion of the inverse hyperbolic sine.

The general interior stretching function for arbitrary t_i is readily obtained from the universal function $w = \sinh z$, by letting $z = iy$. In terms of the range $\Delta y = y_1 - y_0$, and the implicitly defined $\xi_i = \xi(t_i)$, the final result can be written as

$$t = t_i \left\{ 1 + \frac{\sinh [\Delta y (\xi - \xi_i)]}{\sinh \xi_i \Delta y} \right\}. \quad (75)$$

The inverse function is

$$\xi = \xi_i + \frac{1}{\Delta y} \sinh^{-1} [(t/t_i - 1) \sinh \xi_i \Delta y]. \quad (76)$$

The relation between ξ_i and t_i (for a given Δy) is obtained from equation (75) by setting $t = \xi = 1$. The result can be written as

$$\frac{1}{t_i} = 1 - \cosh \Delta y + \sinh \Delta y \coth \xi_i \Delta y. \quad (77)$$

Expressing the inverse hyperbolic cotangent in terms of a logarithm, we can write the inverse of equation (77) as

$$\xi_i = \frac{1}{2\Delta y} \log \left[\frac{1 + t_i (e^{\Delta y} - 1)}{1 - t_i (1 - e^{-\Delta y})} \right]. \quad (78)$$

Equations (76) and (78) are precisely the ones given by Thomas et al. (ref. 7)

If s_i and t_i are the given parameters, the corresponding value of Δy must be calculated. This can be done by differentiating equation (75) and substituting into equation (73). Using equation (77) to eliminate ξ_i , we can write the result as

$$\frac{1}{(s_i t_i \Delta y)^2} = \left[\frac{\cosh \Delta y - 1 + 1/t_i}{\sinh \Delta y} \right]^2 - 1. \quad (79)$$

This is an implicit equation for Δy involving two independent parameters. If the interior point is not too close to either end, and the slope s_i is sufficiently large, one can obtain a simplification. Assuming that $\exp(-2\Delta y) < \ll 1$, we can approximate equation (79) as

$$2s_i \sqrt{t_i (1 - t_i)} \approx \frac{\sinh (\Delta y/2)}{\Delta y/2} . \quad (80)$$

Equation (80) is in the form of equation (62), and one can use the approximate analytic inversion derived in Appendix B.

The special case of an anti-symmetric solution is obtained by setting $t_i = \xi_i = 1/2$. The results (derived in Appendix E) are

$$t = 1/2 \left\{ 1 + \frac{\sinh [\Delta y(\xi - 1/2)]}{\sinh (\Delta y/2)} \right\} \quad (81)$$

$$\text{and } \xi = 1/2 + \frac{1}{\Delta y} \sinh^{-1} [(2t-1)\sinh(\Delta y/2)], \quad (82)$$

$$\text{where } s_i = s_{1/2} = \frac{\sinh (\Delta y/2)}{\Delta y/2} . \quad (83)$$

A one-sided stretching function is obtained by setting $t_i = \xi_i = 0$. The results can be written as

$$t = \frac{\sinh (\xi \Delta y)}{\sinh \Delta y} \quad (84)$$

$$\text{and } \xi = \frac{1}{\Delta y} \sinh^{-1}(t \sinh \Delta y), \quad (85)$$

$$\text{where } s_i = s_0 = \frac{\sinh \Delta y}{\Delta y} . \quad (86)$$

It is interesting to compare the one-sided stretching function derived from the hyperbolic tangent (equations (54) to (56)) with the above function derived from the hyperbolic sine. Letting the subscripts T and S stand for the tangent and sine solutions, we see from equations (54) and (86) that for a given s_0 ,

$$2\Delta y_T = \Delta y_S . \quad (87)$$

The maximum inverse length scale $L^{-1}_{t\xi}$ as defined by equation (2) occurs at $t = 0$ for the tangent solution, and has the value

$$((L^{-1}_{t\xi})_{\max})_T = 2\Delta y_T \tanh \Delta y_T . \quad (88)$$

For the sine solution, the maximum occurs at $t = 1$, and has the value

$$((L^{-1}_{t\xi})_{\max})_S = \Delta y_S \tanh \Delta y_S . \quad (89)$$

Thus, for s_0 large enough so that $\tanh \Delta y_T \approx \tanh \Delta y_S \approx 1$, the two solutions have the same maximum inverse length scale. The minimum slope $(d\xi/dt)_{\min}$ occurs at $t = 1$ for both solutions. The results are

$$((d\xi/dt)_{\min})_T = \frac{\tanh \Delta y_T}{\Delta y_T} \quad (90)$$

and
$$((d\xi/dt)_{\min})_S = \frac{\tanh \Delta y_S}{\Delta y_S} . \quad (91)$$

For large s_0 , we thus obtain

$$((d\xi/dt)_{\min})_S \approx 1/2((d\xi/dt)_{\min})_T . \quad (92)$$

The one-sided function derived from the hyperbolic tangent thus has more points at the unclustered end ($t = 1$) than the one derived from the hyperbolic sine, for identical clustering at $t = 0$. The difference is due to the fact that the zero inflection point occurs at $t = 1$ for the first, and $t = 0$ for the second. The particular application would determine which of these two is preferable.

V. CONCLUDING REMARKS

In this work it has been assumed that the metrics and Jacobians that arise in the transformed equations are calculated by finite differences. If the equation $\vec{r}(t)$ of the ξ -coordinate curve is known analytically, and the transformation $t(\xi)$ is also given analytically, then the metrics and Jacobians can be analytically determined from the derivatives $d\vec{r}/dt$ and $dt/d\xi$. The truncation error in the numerical calculation will then be due solely to the finite-difference approximations to the derivatives of ϕ with respect to ξ . When ϕ varies monotonically with t , the optimum transformation would be one in which ξ varied linearly with ϕ , since this would result in zero truncation errors.

In order to compare transformations for the numerical and analytic treatment of Jacobians and metrics, consider a strictly one-dimensional case in which the single unknown u varies monotonically with distance x . Assume a highly localized interior region of rapid variation whose thickness is proportioned to the small parameter ν . A simple example of such a solution is

$$u \sim \tanh(x/\nu), \quad (93)$$

where $x = 0$ in the localized region. This is actually the steady-state solution of Burgers' equation with fixed end conditions. For the analytic treatment of Jacobians and metrics, it follows that $\xi(x)$ should be a scaled portion of the hyperbolic tangent. The analysis of Appendix E, which assumes a numerical treatment of Jacobians and metrics, shows that this choice is completely unsuitable, and instead favors a scaled portion of the inverse hyperbolic sine. If the differential equation is written so that only derivatives of u appear, then the hyperbolic tangent transformation should lead to a numerical solution with no truncation errors. But the equation can also be written in a form involving derivatives of several functions of u . An example is a strong conservation form. In this situation one has several variables

$\phi(\xi)$ to be approximated by finite differences, and no single transformation $t(\xi)$ is optimum for all of them. If ν is very small, the hyperbolic tangent transformation would put all the interior grid points inside the region of rapid variation. There would be no points to resolve the boundary of this region. By contrast, the inverse hyperbolic sine transformation puts a sufficient number of points outside the region of rapid variation to resolve the complete one-dimensional region.

The above discussion indicates that there are special situations and forms of the differential equations for which an analytic treatment of Jacobians and metrics can provide a desired accuracy with fewer grid points than the numerical treatment. These cases appear to be restricted to monotonic distributions that can be approximated by simple analytic expressions. For general applications of one-dimensional stretching functions, these special situations will not be met. It is then best to treat the Jacobians and metrics numerically, and use the stretching functions derived in Sections III and IV.

Another assumption in the derivation of the stretching functions is that the dimensionless length scale of the localized region of rapid variation could be extremely small. This requires the dimensionless slope of the transformation $d\xi/dt$ to be extremely large. If this condition is not encountered, and transformation slopes remain of $O(1)$, then the form of the stretching function is not critical. For example, many authors have used a scaled exponential as a one-sided stretching function. This is perfectly reasonable as long as the one-sided slope s_0 is not much larger than one. But one can readily show that the maximum inverse length scale is $\exp(s_0)$ for large s_0 . Thus a simple exponential does not yield a suitable one-sided stretching function for very large slopes.

It should be made clear that Roberts was not the first one to use a stretching function involving the hyperbolic tangent. Mehta and Lavan (ref. 10), in an investigation of flow in a two-dimensional channel with a rectangular cavity, used a transformation based on the hyperbolic tangent to transform a semi-infinite region into a finite computational region, and to cluster grid points at the corners of the cavity. The

maximum dimensionless slope, based on the length of the cavity, had a value of .8664 in their calculations. The transformation would have been a poor one if they had required a very large slope at the corner, as shown in Appendix E. The same authors (ref. 11) used a stretching function based on the inverse hyperbolic tangent in a study of the two-dimensional flow around an airfoil. A previous transformation had transformed the region external to the airfoil into a unit circle. The stretching function was necessary to cluster points further near the airfoil surface (to capture the boundary layer) as well as the free stream (to overcome the stretched grid produced by the first transformation). In their calculation, the non-dimensional slopes at the two ends were 5.77 and 27.8. In this instance, the use of the hyperbolic tangent was both appropriate and necessary, as shown by the analysis of Section III.

An important criterion in the development of a two-sided stretching function is a continuous behavior as s_0 and s_1 varied from zero to infinity. This is necessary to obtain smooth grids constructed algebraically using one-dimensional stretching functions. For $B > 1$, the required function was found to be based on the inverse hyperbolic tangent. At first glance, the same function could be used for $B < 1$, simply by interchanging ξ and t in the expression. (This is what was actually done in the earlier stages of this work). But this would violate the desired continuous behavior in the neighborhood of $B = 1$. The analytic continuation of the inverse hyperbolic tangent is the inverse tangent, which differs from the hyperbolic tangent. One can actually construct anti-symmetric function which are self invertible in this sense, but they do not include the elementary functions, and therefore would not be useful as stretching functions. Since the inverse tangent is not self invertible, it is necessary to use two different representations in calculating the stretching function numerically.

The use of the stretching functions derived in this work requires specifying their slopes at one or two points. The values are either obtained from matching slopes with another function, or estimating the length scale of a localized region where an appropriate dependent variable

undergoes rapid variation. Admittedly, in a complex situation, the derivation of an appropriate length scale is not easy, and the value to assign to the slope can be somewhat arbitrary. Nevertheless, if a consistent criterion is used in assigning slope values, useful grids for numerical calculations can be generated. A recent example of a complex grid which was generated using the general two-sided stretching function is found in reference 12.

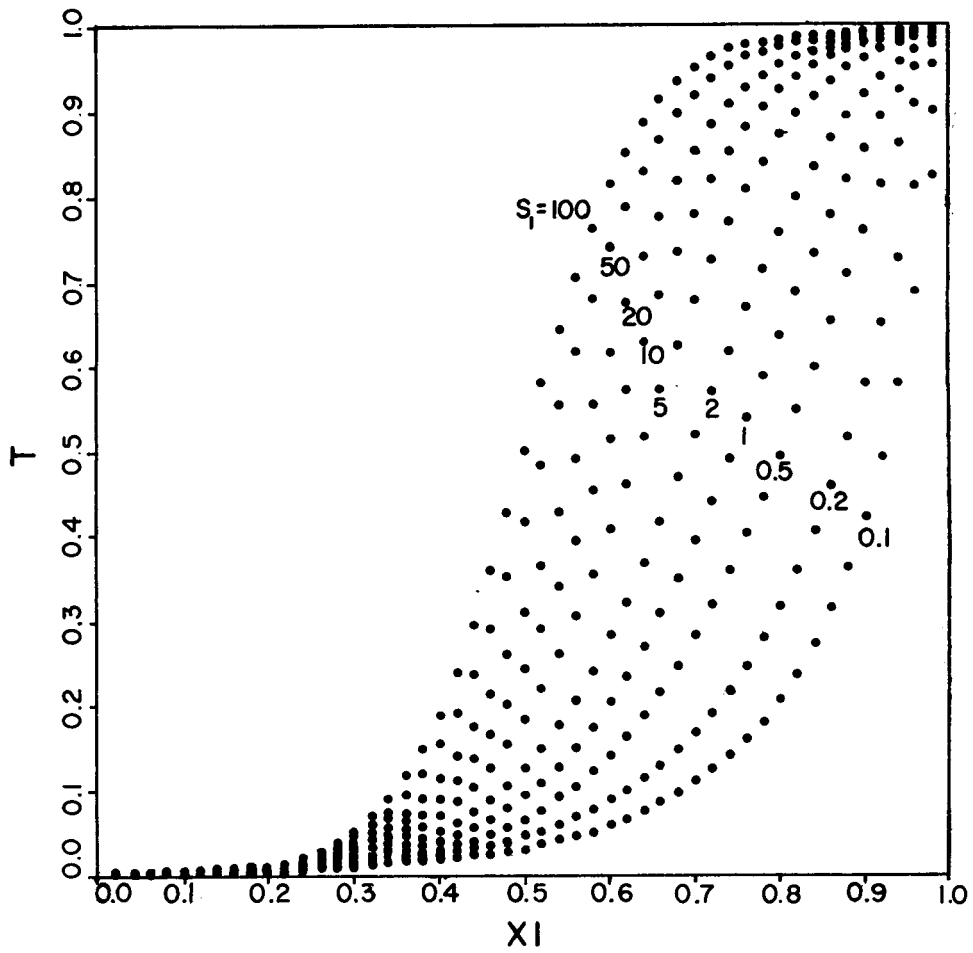


FIGURE 1 TWO-SIDED STRETCHING FUNCTION FOR $S_0 = 100$ AND DIFFERENT VALUES OF S_1 .

VI. REFERENCES

1. Gough, D.O., Spiegel, E.A., and Toomre, J., "Highly Stretched Meshes as Functionals of Solutions", Proceedings of the Fourth International Conference on Numerical Methods in Fluid Dynamics, Springer-Verlag, pp. 191-196, 1975.
2. Ablow, C.M., and Schechter, S., "Campylotropic Coordinates", J. Comp. Phys., Vol. 27(3), pp. 351-362, June 1978.
3. Pierson, B.L., and Kutler, P., "Optimal Nodal Point Distribution for Improved Accuracy in Computational Fluid Dynamics", AIAA J., Vol. 18(1), pp. 49-54, January 1980.
4. Thompson, J.F., Thames, F.C., and Mastin, C.W., "TOMCAT- A Code for Numerical Generation of Boundary-Fitted Curvilinear Coordinate Systems on Fields Containing Any Number of Arbitrary Two-Dimensional Bodies", J. Comp. Phys., Vol. 24(3), pp. 274-302, July 1977.
5. Middlecoff, J.F., and Thomas, P.D., "Direct Control of the Grid Point Distribution in Meshes Generated by Elliptic Equations", Proceedings of the AIAA Fourth Computational Fluid Dynamics Conference, Williamsburg, Virginia, pp. 175-179, July 23-25, 1979.
6. Steger, J.L., and Sorenson, R.L., "Automatic Mesh-Point Clustering Near a Boundary in Grid Generation With Elliptic Partial Differential Equations", J. Comp. Phys., Vol. 33(3), pp.405-410, December 1979.
7. Thomas, P.D., Vinokur, M., Bastianon, R.A., and Conti, R.J., "Numerical Solution for Three-Dimensional Inviscid Supersonic Flow", AIAA J., Vol. 10(7), pp. 887-894, July 1972.
8. Roberts, G.O., "Computational Meshes for Boundary Layer Problems", Proceedings of the Second International Conference on Numerical Methods in Fluid Dynamics", Springer-Verlag, pp. 171-177, 1971.
9. Vinokur, M., Steger, J.L., and Pulliam, T.H., "On Use of Warped Spherical Coordinates to Generate Well Ordered Finite-Difference Grids for Wing-Body Flows. Open Forum, AIAA 11th Fluid and Plasma Dynamics Conference, Seattle, Washington, July 10-12, 1978.
10. Mehta, U.B., and Lavan, Z., "Flow in a Two-Dimensional Channel with a Rectangular Cavity, J. Appl. Mech., Vol. 36, Series E, No. 4, pp. 897-901, December 1969.
11. Mehta, U.B., and Lavan, Z., "Starting Vortex, Separation Bubbles and Stall: A Numerical Study of Laminar Unsteady Flow Around an Airfoil". J. Fluid Mech., Vol. 67(2), pp. 227-256, 1975.
12. Lombard, C.K., Davy, W.C., and Green, M.J., "Forebody and Base Region Real-Gas Flow in Severe Planetary Entry by a Factored Implicit Numerical Method- Part I (Computational Fluid Dynamics). AIAA Paper No. 80-0065, AIAA 18th Aerospace Sciences Meeting, Pasadena, California, January 14-16, 1980.

APPENDIX A

EVALUATION OF ANTI-SYMMETRIC TWO-SIDED STRETCHING FUNCTIONS

In this appendix we evaluate several candidates for an anti-symmetric two-sided stretching function $\xi(t)$, where ξ and t are normalized variables ranging from zero to one. The common slopes at the ends will be designated as

$$B = \frac{d\xi}{dt} (0) = \frac{d\xi}{dt} (1) \quad (A.1)$$

The truncation error analysis of Section II results in the conditions

$$L^{-1} t_{\xi} = \left| \frac{d^2 t}{d\xi^2} \bigg/ \frac{dt}{d\xi} \right| = \left| \frac{d^2 \xi}{dt^2} \bigg/ \left(\frac{d\xi}{dt} \right)^2 \right| = 0 \quad (1) \quad (A.2)$$

and

$$\bar{L}^{-1} t_{\xi} = \left| \frac{d^3 t}{d\xi^3} \bigg/ \frac{dt}{d\xi} \right|^{\frac{1}{2}} = \left| \frac{d^3 \xi}{dt^3} \bigg/ \left(\frac{d\xi}{dt} \right)^3 - 3L^{-2} t_{\xi} \right|^{\frac{1}{2}} = 0(1), \quad (A.3)$$

even if B is very large. The corresponding portion of a universal odd function $w(z)$ ranges from $z_0 = -\Delta z/2$ to $z_1 = \Delta z/2$, where Δz is the total range, and z is either real or pure imaginary. The stretching function is therefore defined as either

$$\xi - \frac{1}{2} = \frac{w \left[\Delta z \left(t - \frac{1}{2} \right) \right]}{2 w \left(\Delta z/2 \right)} \quad (A.4)$$

or

$$t - \frac{1}{2} = \frac{w \left[\Delta z \left(\xi - \frac{1}{2} \right) \right]}{2 w \left(\Delta z/2 \right)} \quad (A.5)$$

Since conditions (A.2) and (A.3) are difficult to satisfy only for very large B , we restrict the analysis to the case $B > 1$.

$$w = \sin z$$

If we let z be real, so that $\Delta z = \Delta x$, the appropriate function $B > 1$ is obtained from equation (A.5) as

$$t - \frac{1}{2} = \frac{\sin [\Delta x (\xi - \frac{1}{2})]}{2 \sin (\Delta x / 2)}. \quad (\text{A.6})$$

Using equation (A.1), we obtain the relation

$$B = \frac{\tan (\Delta x / 2)}{\Delta x / 2}. \quad (\text{A.7})$$

The inverse length scale $L^{-1}_{t\xi}$ takes the form

$$L^{-1}_{t\xi} = \Delta x \left| \tan \left[\Delta x \left(\xi - \frac{1}{2} \right) \right] \right|, \quad (\text{A.8})$$

and has a maximum value

$$(L^{-1}_{t\xi})_{\max} = \Delta x \tan (\Delta x / 2). \quad (\text{A.9})$$

For large B , $\Delta x \rightarrow \pi$, and we obtain

$$(L^{-1}_{t\xi})_{\max} \rightarrow \pi^2 B / 2. \quad (\text{A.10})$$

Thus equation (A.2) is violated, and the function (A.6) is not suitable.

If we let z be imaginary, so that $\Delta z = i\Delta y$, the appropriate function for $B > 1$ is obtained from equation (A.4) as

$$\xi - \frac{1}{2} = \frac{\sinh [\Delta y (t - \frac{1}{2})]}{\sinh (\Delta y / 2)}. \quad (\text{A.11})$$

Applying equation (A.1), we obtain the relation

$$B = \frac{\Delta y / 2}{\tanh (\Delta y / 2)}. \quad (\text{A.12})$$

The inverse length scale $L^{-1}_{t\xi}$ is now

$$L^{-1}_{t\xi} = \frac{2 \sinh(\Delta y/2) |\sinh [\Delta y (t - \frac{1}{2})]|}{1 + \sinh [\Delta y (t - \frac{1}{2})]} \quad (A.13)$$

The maximum value of $L^{-1}_{t\xi}$ is readily found to be

$$(L^{-1}_{t\xi})_{\max} = \sinh (\Delta y/2). \quad (A.14)$$

For large B, $\Delta y/2 \rightarrow B$, and we obtain

$$(L^{-1}_{t\xi})_{\max} \rightarrow \sinh B \sim e^{B/2}. \quad (A.15)$$

Since the maximum inverse length scale becomes exponentially large, the function (A.11) is completely unsuitable.

w = tanz

The appropriate function for real z is obtained from equation (A.4) as

$$\xi - \frac{1}{2} = \frac{\tan [\Delta x (t - \frac{1}{2})]}{2 \tan (\Delta x/2)}. \quad (A.16)$$

The relation of B to Δx is obtained from equation (A.1) as

$$B = \Delta x / \sin \Delta x. \quad (A.17)$$

The inverse length scale $L^{-1}_{t\xi}$ is found to be

$$L^{-1}_{t\xi} = 2 \tan (\Delta x/2) |\sin [\Delta x (2t - 1)]|. \quad (A.18)$$

For $B > \pi/2$, the maximum value of $L^{-1}_{t\xi}$ is given by

$$(L^{-1}_{t\xi})_{\max} = 2 \tan (\Delta x/2). \quad (A.19)$$

For large B, $\Delta x \rightarrow \pi$, and equation (A.17) can be rewritten as

$$B = \frac{\Delta x}{2 \sin(\Delta x/2) \cos(\Delta x/2)} \rightarrow (\pi/2) \tan(\Delta x/2). \quad (\text{A.20})$$

We thus find that

$$(L^{-1}_{t\xi})_{\max} \rightarrow 4B/\pi \quad (\text{A.21})$$

and consequently the function (A.16) is also not suitable.

The corresponding function for imaginary z is obtained from equation (A.5) as

$$t - 1/2 = \frac{\tanh[\Delta y(\xi - 1/2)]}{2 \tanh(\Delta y/2)}. \quad (\text{A.22})$$

The parameter B is now related to Δy by

$$B = \frac{\sinh \Delta y}{\Delta y}. \quad (\text{A.23})$$

The inverse length scale $L^{-1}_{t\xi}$ becomes

$$L^{-1}_{t\xi} = 2\Delta y |\tanh[\Delta y(\xi - 1/2)]|, \quad (\text{A.24})$$

and has the maximum value

$$(L^{-1}_{t\xi})_{\max} = 2\Delta y \tanh(\Delta y/2). \quad (\text{A.25})$$

For large B, equation (A.23) can be inverted approximately to yield

$$\Delta y \rightarrow \log(2B \log B). \quad (\text{A.26})$$

(A more accurate relation is derived in Appendix B.) For sufficiently large B, although Δy is logarithmically of $O(1)$, it is large enough for $\tanh(\Delta y/2) \rightarrow 1$. Consequently we obtain

$$(L^{-1}_{t\xi})_{\max} \rightarrow 2\Delta y \sim 2 \log (2B \log B). \quad (\text{A.27})$$

Thus $L^{-1}_{t\xi}$ remains logarithmically of $O(1)$, even when B becomes extremely large. (For example, if $B = 1101$, $(L^{-1}_{t\xi})_{\max} = 20$.) Condition (A.3) requires the determination of $\bar{L}^{-1}_{t\xi}$, which is given by

$$\bar{L}^{-1}_{t\xi} = \sqrt{2\Delta y} \left| 3 \tanh^2 [\Delta y(\xi - 1/2)] - 1 \right|^{1/2}. \quad (\text{A.28})$$

It follows readily for large B that

$$(\bar{L}^{-1}_{t\xi})_{\max} \approx (L^{-1}_{t\xi})_{\max}, \quad (\text{A.29})$$

and condition (A.3) is also satisfied. The function (A.22) is thus a suitable candidate for a stretching function.

w = erfz

The appropriate function for real z is obtained from equation (A.5) as

$$t - 1/2 = \frac{\text{erf} [\Delta x(\xi - 1/2)]}{2 \text{erf} (\Delta x/2)}. \quad (\text{A.30})$$

Using equation (A.1), we obtain the relation

$$B = \frac{\sqrt{\pi} \text{erf} (\Delta x/2) e^{\Delta x^2/4}}{\Delta x}. \quad (\text{A.31})$$

The inverse length scale $L^{-1}_{t\xi}$ has the simple form

$$L^{-1}_{t\xi} = 2\Delta x^2 |\xi - 1/2|, \quad (\text{A.32})$$

and has the maximum value

$$(L^{-1}_{t\xi})_{\max} = \Delta x^2. \quad (\text{A.33})$$

Approximate inversion of equation (A.31) for large B results in

$$\Delta x^2 \rightarrow 4 \log [2B(\log B/\pi)^{1/2}]. \quad (\text{A.34})$$

We again find that $L^{-1}_{t\xi}$ is logarithmically of $O(1)$, and can also show that $(\bar{L}^{-1}_{t\xi})_{\max} \approx (L^{-1}_{t\xi})_{\max}$. The error function is not as simple as the hyperbolic tangent, and is not invertible. Furthermore, for a given value of B, the maximum inverse length scale for the error function is larger than that for the hyperbolic tangent. Thus the function (A.22) is the best candidate for a simple, anti-symmetric, two-sided stretching function.

APPENDIX B
INVERSION OF $y = \sinh x/x$

Given the function

$$y = \sinh x/x, \tag{B.1}$$

we seek an approximate inverse function $x = f(y)$ for $y > 1$. The accuracy of the approximation will be measured by calculating the fractional error in y , given by

$$\text{error}(y) = \frac{\sinh[f(y)]}{yf(y)} - 1. \tag{B.2}$$

An expansion for $f(y)$ near $y = 1$ is readily obtained, but it has a small radius of convergence. An asymptotic expansion for large y is found to converge very slowly. The range of y for which a high accuracy is required extends to $y \sim 100$. A maximum absolute error of .0005 is probably sufficient for the numerical applications of this function. Hopefully, these criteria can be satisfied by matching appropriate expansions for small and large y with the exact solution at some intermediate point y_1 . Since the asymptotic expansion has slow convergence, it will also be matched to the exact solution at another point y_2 . An outline of the derivation of the two expansions will now be presented.

For given values of x_1 and x_2 , the corresponding values of y_1 , y_2 , $(dx/dy)_1$, $(d^2x/dy^2)_1$, and $(dx/dy)_2$ are obtained from equation (B.1) by substitution and implicit differentiation. We first consider the expansion for $y < y_1$. Since $y \sim 1 + x^2/6$ for small x , $f(y) \sim \sqrt{6(y-1)}$ for y near one. If we introduce the variable

$$\bar{y} = y - 1, \tag{B.3}$$

we can write an expansion for x in the form

$$x = \sqrt{6\bar{y}} (1 + A_1\bar{y} + A_2\bar{y}^2 + A_3\bar{y}^3 + A_4\bar{y}^4 + A_5\bar{y}^5). \tag{B.4}$$

The coefficients A_1 and A_2 are determined by inverting the expansion of equation (B.1) for small x and equating coefficients of \bar{y} . The results are

$$A_1 = -.15 \quad (B.5)$$

and

$$A_2 = \frac{3 \times 107}{32 \times 175}. \quad (B.6)$$

By differentiating equation (B.4), we can set x , dx/dy , and d^2x/dy^2 equal to their known exact values at \bar{y}_1 . The resultant three simultaneous linear algebraic equations are readily solved for A_3 , A_4 and A_5 .

In order to obtain the expansion for $y > y_1$, we must first determine the leading terms in the asymptotic expansion for large x . Equation (B.1) can be rewritten as

$$x = \sinh^{-1}(xy). \quad (B.7)$$

Since $\sinh^{-1} z \sim \log(2z)$ asymptotically for large z , we obtain the asymptotic expression

$$x \sim v + \log(2x) \quad (B.8)$$

where

$$v = \log y. \quad (B.9)$$

Substituting the zeroth order approximation

$$x^{(0)} \sim v \tag{B.10}$$

into equation (B.8), we obtain the next approximation

$$x^{(1)} \sim v + \log(2v). \tag{B.11}$$

The further substitution of $x^{(1)}$ into equation (B.8) results in

$$x^{(2)} \sim v + \log[2v(1 + \log(2v)/v)] \\ \sim v + \log(2v) + \log(2v)/v$$

or
$$x^{(2)} \sim v + (1 + 1/v) \log(2v). \tag{B.12}$$

The asymptotic approximation (B.12) agrees very well with the exact solution for $y \geq 1$, giving a maximum absolute error of .02 occurring at $y \sim 200$. The next higher order approximation gives poorer results in our range of interest. In order to obtain better accuracy, and join the solution with the expansion for small y , we add a polynomial in inverse powers of y . Since we will also match exact conditions at y_2 , it is more reasonable to define instead the variable

$$w = 1/y - 1/y_2. \tag{B.13}$$

The expansion for x is thus taken to be

$$x = v + (1+1/v) \log(2v) + B_0 + B_1 w + B_2 w^2 + B_3 w^3 + B_4 w^4. \tag{B.14}$$

The coefficients B_0 and B_1 are determined by equating x and dx/dy to their known exact values at y_2 . Similarly, the coefficients B_2 , B_3 and B_4 are obtained by equating x , dx/dy , and d^2x/dy^2 to their known values at y_1 .

For fixed y_1 and y_2 , as y increase above one, the error determined by equations (B.2) and (B.4) becomes positive, reaches a maximum, and decreases to zero at y_1 . Using equation (B.14), we find that the error becomes positive again beyond y_1 , reaches a maximum, decreases through zero, reaches a minimum (which is negative), and increases to zero at y_2 . Beyond y_2 the error grows monotonically negative. Thus the absolute error reaches a local maximum three times in the range $1 < y < y_2$. The optimum choice of y_1 and y_2 is that which makes these three maxima equal. By a trial and error procedure, this condition was found for the values $x_1 = 2.722567$ and $x_2 = 6.05012$, corresponding to $y_1 = 2.7829681$ and $y_2 = 35.053980$. The corresponding maximum absolute error is .000267732, which is more than sufficient. This value is again reached at $y = 69.64$. The magnitude of the error increases beyond this, reaching .0006 at $y \sim 100$ and .00083 at $y = 120.5$. Thus, the desired criteria are essentially satisfied by the two approximations. The numerical values for the final coefficients are given by equations (65) and (67).

APPENDIX C

INVERSION OF $y = \sin x/x$

Given the function

$$y = \sin x/x, \tag{C.1}$$

we seek an approximate inverse function $x = g(y)$ in the range $0 < y < 1$. The accuracy of the approximation will be measured by calculating the fractional error in y , given by

$$\text{error}(y) = \frac{\sin [g(y)]}{yg(y)} - 1. \tag{C.2}$$

The approximation is derived by matching appropriate expansions for y near zero and y near one with the exact solution at some intermediate point y_1 . The derivation is briefly outlined below.

For a given x_1 , the corresponding values of y_1 , $(dx/dy)_1$, and $(d^2x/dy^2)_1$, are obtained from equations (C.1) by substitution and implicit differentiation. The approximation for $y < y_1$ utilizes the expansion of equation (C.1) near $y = 0$, as a polynomial in powers of $\pi - x$. Based on the inversion of this expansion, we take for an approximation the expression

$$x = \pi [1 - y + y^2 - (1 + \pi^2/6) y^3 + B_4 y^4 + B_5 y^5 + B_6 y^6]. \tag{C.3}$$

By differentiating equation (C.3), we can set x , dx/dy , and d^2x/dy^2 equal to their known exact values at y_1 . The resultant three simultaneous linear algebraic equations are readily solved for B_4 , B_5 and B_6 .

The approximation for $y > y_1$ similarly utilizes the expansion of equation (C.1) near $y = 1$. Introducing the variable

$$\bar{y} = 1 - y, \tag{C.4}$$

we obtain an approximation in the form

$$x = \sqrt{6\bar{y}} (1 + A_1\bar{y} + A_2\bar{y}^2 + A_3\bar{y}^3 + A_4\bar{y}^4 + A_5\bar{y}^5). \quad (C.5)$$

The coefficients A_1 and A_2 obtained from the expansion near $y = 1$ are

$$A_1 = .15 \quad (C.6)$$

and

$$A_2 = \frac{3 \times 107}{32 \times 175} . \quad (C.7)$$

The coefficients A_3 , A_4 and A_5 are obtained by equating x , dx/dy , and d^2x/dy^2 to their known values at y_1 .

The error defined by equation (C.2) reaches a local maximum between $y = 0$ and $y = y_1$, and a local minimum (which is negative) between $y = y_1$ and $y = 1$. The optimum choice of y_1 will make the magnitudes of these extrema equal. This was found by trial and error to be produced by $x_1 = 2.428464$ (corresponding to $y_1 = .26938972$). The maximum absolute error is .000197170, which is more than sufficient for numerical calculations. The numerical values for the final coefficients are given by equations (71) and (72).

APPENDIX D

SOLUTION CHARACTERISTICS OF THE TWO-SIDED STRETCHING FUNCTION DERIVED FROM $w = \tanz$

In this appendix we study the two-sided stretching function derived from

$$w = \tanz, \quad (D.1)$$

where z is the complex variable

$$z = x + iy. \quad (D.2)$$

If z_0 and z_1 are the two end points of the solution in the z -plane which define the range

$$\Delta z = z_1 - z_0, \quad (D.3)$$

it is shown in Section III that the appropriate variables for the stretching function are defined as

$$\xi = (z - z_0)/\Delta z \quad (D.4)$$

and

$$t = (\tanz - \tanz_0)/(\tanz_1 - \tanz_0), \quad (D.5)$$

while the governing parameters A and B are related to z_0 and z_1 , through

$$B = \sin\Delta z/\Delta z \quad (D.6)$$

and

$$A = \frac{\cos z_0}{\cos z_1}. \quad (D.7)$$

Using equation (D.3), A can also be expressed in the form

$$1/A = \cos \Delta z - \tan z_0 \sin \Delta z. \quad (D.8)$$

It is also useful to express $\tan z_0$ as a complex number in the form

$$\tan z_0 = \frac{\sin 2x_0 + i \sinh 2y_0}{\cos 2x_0 + \cosh 2y_0}. \quad (D.9)$$

We will first study the real representations of the solution for various ranges of A and B. If $B < 1$, it follows from equation (D.6) that Δz is real. Using equations (D.8), (D.9), and (D.4), one can prove that $\tan z_0$, z_0 , and z are all real. The stretching function is thus a scaled portion of

$$w = \tan x. \quad (D.10)$$

This representation breaks down as $B \rightarrow 1$, since $\Delta z \rightarrow 0$. For $A \gtrsim 1$, it follows from equation (D.8) and (D.7) that $z \rightarrow \pm \pi/2$. We can obtain the correct representation in the limit by introducing

$$\bar{x} = x \mp \pi/2, \quad (D.11)$$

where $\bar{x} \lesssim 0$. Since $\tan(\bar{x} \pm \pi/2) = -\cot \bar{x} \approx -1/\bar{x}$ as $\bar{x} \rightarrow 0$, it follows that for $B = 1$ the stretching function is a scaled portion of one branch of the rectangular hyperbola

$$w = -1/\bar{x}. \quad (D.12)$$

If $B > 1$, it follows from equation (D.6) that Δz is pure imaginary, i.e. $\Delta x = 0$. From equation (D.4) it then follows that $x = x_0$, so that the real part of z is constant. Since equation (D.8) required $\tan z_0$ to be pure imaginary, one can deduce from equation (D.9) that $x = -\pi/2, 0$, or $+\pi/2$. If A is sufficiently close to one, the appropriate solution is $x = 0$, and equation (D.1) becomes

$$w = i \tanh y. \quad (D.13)$$

Thus the stretching function is a scaled portion of the hyperbolic tangent. As A departs from one, this representation must break down. One can easily show from equation (D.8) that as $A \rightarrow \exp(-\Delta y)$, $y_0 \rightarrow +\infty$ and as $A \rightarrow \exp(\Delta y)$, $y_0 \rightarrow -\infty$. Since $|y| \rightarrow \infty$ in these two cases, equation (D.13) takes the limiting form

$$w = \pm i(1 - 2e^{-2|y|}). \quad (D.14)$$

The stretching function then becomes a scaled portion of an exponential. This limit is reached when B attains the critical value

$$B^* = \frac{\sinh |\log A|}{\log A}. \quad (D.15)$$

For A near one, equation (D.15) has the approximate form

$$\log B^* = 1/6 (\log A)^2, \quad (D.16)$$

while for $A \gg 1$ and $1/A \gg 1$ we obtain the asymptotic form

$$\log B^* \rightarrow |\log A| - \log (2|\log A|). \quad (D.17)$$

For a fixed $A \gtrsim 1$, as B decreases below B^* ; the appropriate solution for z is

$$z = \frac{\pm \pi}{2} + iy. \quad (D.18)$$

The sign of the correct branch follows from equation (D.11) by taking the limit $B \rightarrow 1$. Equation (D.1) then becomes

$$w = \text{icothy}. \quad (D.19)$$

Thus, for $1 < B < B^*$, the stretching function is a scaled portion of one branch of the hyperbolic cotangent. The boundaries for the various real representations of the solution are shown in figure D.1, which is a log-log plot of the B vs A plane.

Another interesting property is to determine the conditions under which the solution curve contains an inflection point. This is certainly true for the anti-symmetric curve ($A = 1$). As A departs from one, the inflection point moves towards one end, and eventually could disappear. The critical point is reached when either $z_1 = 0$ or $z_0 = 0$. From equations (D.3) and (D.7), it follows that the former condition occurs when

$$A = \cos \Delta z. \quad (D.20)$$

The inflection point thus occurs at the right end of the curve when B attains the critical value

$$B^+ = \sqrt{A^2 - 1} / \cosh^{-1} A \quad (A > 1) \quad (D.21a)$$

and

$$B^+ = \sqrt{1 - A^2} / \cos^{-1} A \quad (A < 1). \quad (D.21b)$$

For A near one, equation (D.21) has the approximate form

$$\log B^+ = 1/3 \log A, \quad (D.22)$$

while for $A \gg 1$ we obtain from equation (D.21a) the asymptotic form

$$\log B^+ \rightarrow \log 2A - \log (2 \log 2A). \quad (D.23)$$

It also follows from equation (D.21b) that $A \rightarrow 0$, B^+ attains the minimum value

$$B_{\min} = 2/\pi. \quad (D.24)$$

The condition $z_0 = 0$ is found to occur when

$$A = 1/\cos \Delta z. \quad (D.25)$$

Thus the inflection point occurs at the left end of the curve when B attains the critical value

$$B^- = \sqrt{1 - 1/(A^2)} / \cos^{-1}(1/A) \quad (A > 1) \quad (D.26a)$$

and

$$B^- = \sqrt{1/(A^2) - 1} / \cosh^{-1}(1/A) \quad (A < 1). \quad (D.26b)$$

For A near one, equation (D.26) has the approximate form

$$\log B^- = -1/3 \log A, \quad (D.27)$$

while for $A \ll 1$, we obtain from equation (D.26b) the asymptotic form

$$\log B^- \rightarrow -\log(A/2) - \log(-2 \log(A/2)). \quad (D.28)$$

Condition (D.24) is again reached when $A \rightarrow \infty$.

From the above relations, one can conclude that the solution curve contains an inflection point unless B lies between B^+ and B^- . Alternatively, an inflection point will be present if $1/\cosh\Delta y < A < \cosh\Delta y$ for $B > 1$, and $\cos\Delta x < A < 1/\cos\Delta x$ for $B < 1$. An inflection point must always occur if $B < 2/\pi$. The regions of the B-A plane where the solution curve has inflection points are also shown in figure D.1. Note that these regions do not cover completely the regions where solutions are based on the tangent and hyperbolic tangent. Thus there are narrow ranges for which a solution curve based on the tangent and hyperbolic tangent does not contain an inflection point.

Still another way to study the solution is to follow its path in the complex z-plane. This is best done by finding the locus of the solution for constant B, as A increases from zero to infinity. It is easy to show that as $A \rightarrow 0$, $x_0 \rightarrow -\pi/2$ for all solutions. Similarly, as $A \rightarrow \infty$, $z \rightarrow \pi/2$ for all solutions. The solution paths are shown in figure D.2,

with a dashed line for $B < 1$ and solid line for $B > 1$. The details of the solution histories are presented below.

$B < 1$

Since z is real, the solution remains on the real axis. When $A = 0$, $x_0 = -\pi/2$, and $x_1 = -\pi/2 + \Delta x$. (If $B > 2/\pi$, $x_1 < 0$, and the solution has no inflection point). As A increases, both x_0 and x_1 increase. (If $B > 2/\pi$, $x_1 = 0$ and an inflection point appears when $A = \cos \Delta x$). When $A = 1$, $x_0 = -\Delta x/2$, $x_1 = \Delta x/2$, and we have the anti-symmetric solution. (If $B > 2/\pi$, $x_0 = 0$ and the inflection point disappears when $A = 1/\cos \Delta x$). When A reaches $+\infty$, $x_1 = \pi/2$, and $x_0 = \pi/2 - \Delta x$.

$B > 1$

With $\Delta z = i\Delta y$, the solution at $A = 0$ has $z_0 = -\pi/2$, and $z_1 = -\pi/2 + i\Delta y$. As A increases, the solution stays on the line $x = -\pi/2$, and both y_0 and y_1 increase. When $A = \exp(-\Delta y)$, $y_0 = y_1 = +\infty$. As A increases beyond $\exp(-\Delta y)$, the solution returns along the imaginary axis, and both y_0 and y_1 decrease from $+\infty$. When $A = 1/\cosh \Delta y$, $y_0 = 0$, and an inflection point first appears. When $A = 1$, $y_0 = -\Delta y/2$, $y_1 = \Delta y/2$, and we have the anti-symmetric solution. When $A = \cosh \Delta y$, $y_1 = 0$, and the inflection point disappears. When $A = \exp(\Delta y)$, $y_0 = y_1 = -\infty$. As A increases beyond $\exp(\Delta y)$, the solution returns along the line $x = \pi/2$, and both y_0 and y_1 increase from $-\infty$. When A reaches $+\infty$, $z_1 = \pi/2$, and $z_0 = \pi/2 - i\Delta y$.

$B = 1$

When $A = 0$, $z_0 = z_1 = -\pi/2$. As A increases, the solution remains at that point. When $A = 1$, z_0 and z_1 jump to the origin. When $A > 1$, z_0 and z_1 jump to $+\pi/2$, where they remain as A increases to $+\infty$. Since $B = 1$ is the boundary between $B > 1$ and $B < 1$, the solution can occur only at these points where the $B > 1$ and $B < 1$ solutions intersect. As shown in figure D.2, the solid line ($B > 1$) and dashed line ($B < 1$) intersect precisely at the three points defined above.

FIGURE D.1
SOLUTION CHARACTERISTICS OF TWO-
SIDED STRETCHING FUNCTION DERIVED
FROM $W = \tan Z$

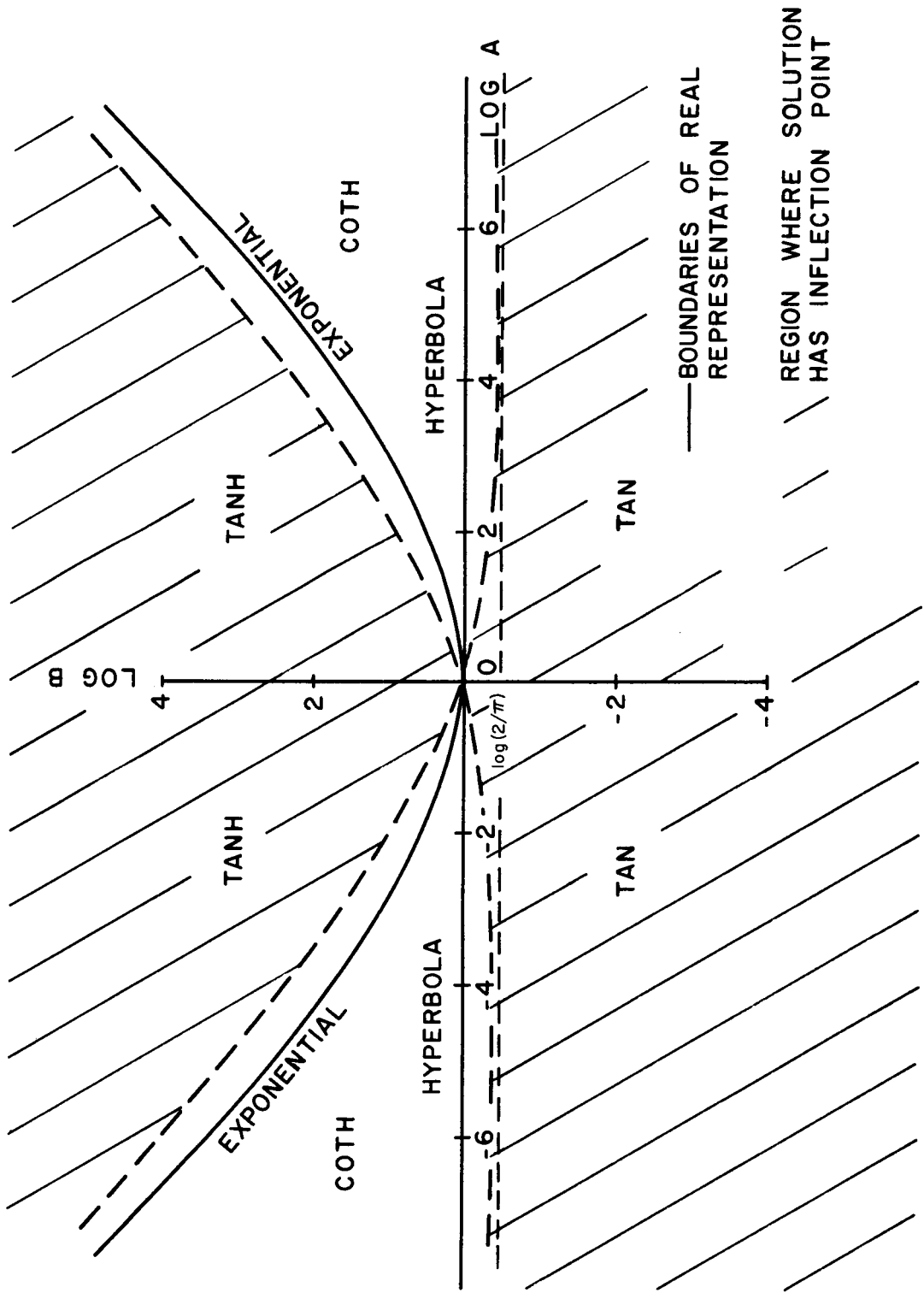
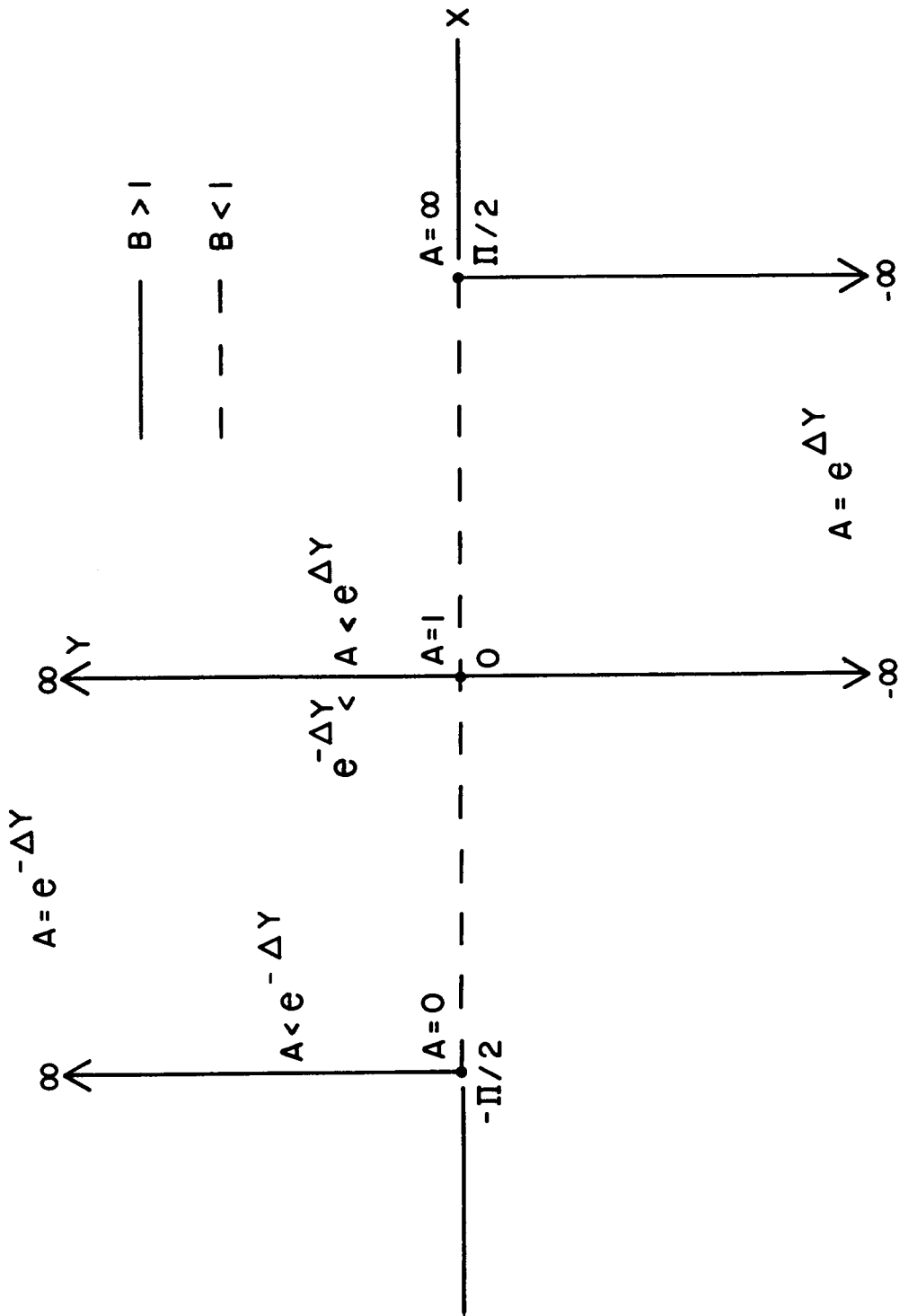


FIGURE D.2: LOCUS OF SOLUTION IN Z-PLANE



APPENDIX E

EVALUATION OF ANTI-SYMMETRIC INTERIOR STRETCHING FUNCTIONS

In this appendix we evaluate several candidates for an anti-symmetric interior stretching function $\xi(t)$, where ξ and t are normalized variables ranging from zero to one. The slope at the midpoint will be designated as

$$B = \frac{d\xi}{dt} (1/2), \quad (E.1)$$

and only the case $B > 1$ will be considered. The criteria to be satisfied are that the inverse length scales $L_{t\xi}^{-1}$ and $L_{t\xi}^{-1}$ (defined in Appendix A, equations (A.2) and (A.3)) be of order one, even if B is very large. We seek a solution that is a scaled portion of a universal odd function $w(z)$. In terms of the range Δz , expressions for ξ or t are given by equations (A.4) or (A.5).

$$w = \tanh z$$

If we let z be real, so that $\Delta z = \Delta x$, the appropriate function for $B > 1$ is obtained from equation (A.5) as

$$t - 1/2 = \frac{\tan [\Delta x(\xi - 1/2)]}{2 \tan (\Delta x/2)}. \quad (E.2)$$

Using equation (B.1) we obtain the relation

$$B = \frac{\tan (\Delta x/2)}{\Delta x/2}. \quad (E.3)$$

The inverse length scale $L_{t\xi}^{-1}$ takes the form

$$L_{t\xi}^{-1} = 2\Delta x |\tan [\Delta x(\xi - 1/2)]|, \quad (E.4)$$

and has a maximum value

$$(L_{t\xi}^{-1})_{\max} = 2\Delta x \tan (\Delta x/2). \quad (E.5)$$

For large B, $\Delta x \rightarrow \pi$ and we obtain

$$(L^{-1}_{t\xi})_{\max} \rightarrow \pi^2 B. \quad (E.6)$$

Since the inverse length scale is proportioned to B, the function (E.2) is not suitable.

If we let z be imaginary, so that $\Delta z = i\Delta y$, the appropriate function for $B > 1$ is obtained from equation (A.4) as

$$\xi - 1/2 = \frac{\tanh [\Delta y(t-1/2)]}{2 \tanh (\Delta y/2)}. \quad (E.7)$$

Applying equation (E.1), we obtain the relation

$$B = \frac{\Delta y/2}{\tanh (\Delta y/2)}. \quad (E.8)$$

The inverse length scale $L^{-1}_{t\xi}$ is now

$$L^{-1}_{t\xi} = 2 \tanh (\Delta y/2) |\sinh [\Delta y(2t-1)]|, \quad (E.9)$$

and has a maximum value

$$(L^{-1}_{t\xi})_{\max} = 2 \tanh (\Delta y/2) \sinh \Delta y. \quad (E.10)$$

For large B, $\Delta y/2 \rightarrow B$, $\tanh(\Delta y/2) \rightarrow 1$, and we obtain

$$(L^{-1}_{t\xi})_{\max} \rightarrow 2 \sinh 2B \sim e^{2B}. \quad (E.11)$$

Since the inverse length scale grows exponentially with B, the function (E.7) is completely unsuitable.

w = sinz

The appropriate function for real z is obtained from equation (A.4) as

$$\xi - 1/2 = \frac{\sin [\Delta x (t-1/2)]}{2 \sin (\Delta x/2)} . \quad (E.12)$$

The relation of B to Δx is obtained from equation (E.1) as

$$B = \frac{\Delta x/2}{\sin (\Delta x/2)} . \quad (E.13)$$

Since $\Delta x \leq \pi$ if function (E.12) is to remain monotonic, it follows from equation (E.13) that $B \leq \pi/2$. Therefore a monotonic stretching function for large B cannot be obtained using function (E.12).

The corresponding function for imaginary z is obtained from equation (A.4) as

$$t - 1/2 = \frac{\sinh [\Delta y (\xi-1/2)]}{2 \sinh (\Delta y/2)} . \quad (E.14)$$

The parameter B is now related to Δy by

$$B = \frac{\sinh(\Delta y/2)}{\Delta y/2} . \quad (E.15)$$

The inverse length scale $L^{-1}_{t\xi}$ becomes

$$L^{-1}_{t\xi} = \Delta y \tanh [\Delta y (\xi-1/2)] , \quad (E.16)$$

and has the maximum value

$$(L^{-1}_{t\xi})_{\max} = \Delta y \tanh (\Delta y/2) . \quad (E.17)$$

For large B, equation (E.15) can be inverted approximately to yield

$$\Delta y \rightarrow 2 \log (2B \log B) . \quad (E.18)$$

For sufficiently large B, Δy is large enough for $\tanh (\Delta y/2) \rightarrow 1$. Consequently we obtain

$$(L^{-1}_{t\xi})_{\max} \rightarrow \Delta y \sim 2 \log (2B \log B) . \quad (E.19)$$

Thus $L^{-1}_{t\xi}$ remains logarithmically of $O(1)$, even for very large B . The inverse length scale $\bar{L}^{-1}_{t\xi}$ becomes

$$\bar{L}^{-1}_{t\xi} = \Delta y. \quad (\text{E.20})$$

It follows that for large B

$$(\bar{L}^{-1}_{t\xi})_{\max} \approx (L^{-1}_{t\xi})_{\max}. \quad (\text{E.21})$$

Since both inverse length scales remain of $O(1)$, the function (E.14) is a suitable candidate for a stretching function.

1. Report No. NASA CR-3313		2. Government Accession No.		3. Recipient's Catalog No.	
4. Title and Subtitle On One-Dimensional Stretching Functions for Finite-Difference Calculations				5. Report Date October 1980	
				6. Performing Organization Code	
7. Author(s) Marcel Vinokur, Principal Investigator				8. Performing Organization Report No.	
				10. Work Unit No. 505-31-11-06	
9. Performing Organization Name and Address School of Engineering Engineering and Applied Science Research University of Santa Clara Santa Clara, California				11. Contract or Grant No. NSG-2086	
				13. Type of Report and Period Covered Contractor Report July 1, 1978 to June 30, 1979	
12. Sponsoring Agency Name and Address National Aeronautics and Space Administration Washington, D. C. 20546				14. Sponsoring Agency Code	
15. Supplementary Notes Ames Technical Monitor: Harvard Lomax Final Report					
16. Abstract The class of one-dimensional stretching functions used in finite-difference calculations is studied. For solutions containing a highly localized region of rapid variation, simple criteria for a stretching function are derived using a truncation error analysis. These criteria are used to investigate two types of stretching functions. One is an interior stretching function, for which the location and slope of an interior clustering region are specified. The simplest such function satisfying the criteria is found to be one based on the inverse hyperbolic sine. It was first employed by Thomas et al. The other type of function is a two-sided stretching function, for which the arbitrary slopes at the two ends of the one-dimensional interval are specified. The simplest such general function is found to be one based on the inverse tangent. The special case where the slopes were both equal and greater than one was first employed by Roberts. The general two-sided function has many applications in the construction of finite-difference grids. An example of such an application is found in one of the references.					
17. Key Words (Suggested by Author(s)) Stretching Functions, Grid Clustering, and Finite-Difference Grids			18. Distribution Statement Unclassified - Unlimited Star Category - 64		
19. Security Classif. (of this report) Unclassified		20. Security Classif. (of this page) Unclassified		21. No. of Pages 55	22. Price* A04

*For sale by the National Technical Information Service, Springfield, Virginia 22161

NASA-Langley, 1980